LITHOS

Hercynian granitoids from the Central Iberian Zone (Northern Portugal)

G. Dias [a,*], J. Leterrier [b], A. Mendes [a], P.P. Simões [a], J.M. Bertrand [c]

[a] *Departamento de Ciências da Terra, Universidade do Minho, Campus de Gualtar, 4719 Braga Codex, Portugal*
[b] *Centre de Recherches Pétrographiques et Géochimiques, CNRS, B.P. 20, 54501 Vandoeuvre-lès-Nancy, France*
[c] *Laboratoire de Géodynamique des Chaînes Alpines, B.P. 1104, 73011 Chambery Cedex, France*

Abstract

In the Central Iberian Zone (CIZ) of the Iberian Massif large volumes of granitoids were emplaced during the post-collisional stage of the Hercynian orogeny (syn- to post-D3, the last ductile deformation phase). Twelve granitic units and a quartz monzodiorite were selected for a U–Pb zircon and monazite geochronological study. They represent successive stages of the D3 event. The Ucanha-Vilar, Lamego, Sameiro and Refoios do Lima plutons are coeval (313 ± 2 Ma, 319 ± 4 Ma, 316 ± 2 Ma and 314 ± 2 Ma, respectively) and belong to the earliest stage. Later on the Braga massif was emplaced, its different units yielding the same age: 309 ± 3 Ma for the Braga granite, 309 ± 1 Ma for the Gonça granite and 311 ± 5 Ma for a related quartz monzodiorite. The Braga massif is subcontemporaneous with the Agrela and Celeirós plutons (307 ± 3.5 Ma and 306 ± 2 Ma, respectively), in agreement with field data. The Briteiros granite is younger (300 ± 1 Ma), followed by the emplacement of the Peneda–Gerês massif (Gerês, Paufito, Illa and Carris granites). The Gerês granite, emplaced at 296 ± 2 Ma, seems to represent a first magmatic pulse immediately followed by the intrusion of the Paufito granite at 290 ± 2.5 Ma. For the Carris granite a minimum emplacement age of 280 ± 5 Ma was obtained. Based on these results the following chronology is proposed: (1) syn-D3 biotite granitoids, 313–319 Ma; (2) late-D3 biotite-dominant granitoids, 306–311 Ma; (3) late- to post-D3 granitoids, ca. 300 Ma; (4) post-D3 granitoids, 290–296 Ma. These chronological data indicate that successive granitic intrusions were emplaced in the CIZ during a short time span of about 30 Ma that corresponds to the latest stages of the Hercynian orogeny. A rapid and drastic change occurred at about 300 Ma, between a compressive ductile tectonic regime (D3, ca. 300–320 Ma) associated to calc-alkaline, monzonitic and aluminopotassic plutonism and a fragile phase of deformation (D4) which controlled the emplacement of the subalkaline ferro-potassic plutonism at 290–296 Ma. © 1998 Elsevier Science B.V. All rights reserved.

Keywords: Iberian Peninsula; Hercynian; Granitoids; Zircon; Monazite; U–Pb geochronology

---

* Corresponding author. Fax: +351-53-678206; E-mail: graciete@ci.uminho.pt

1. Introduction

The Iberian Massif is a large segment of the European Hercynian Fold Belt which extends over more than 3000 km from eastern Germany to the Iberian Peninsula. The tectonometamorphic and magmatic features of the European Hercynian Belt have been explained by an obduction–collision orogenic model (Bard et al., 1980; Matte, 1986; Lagarde et al., 1992; Burg et al., 1994; Rey et al., 1997). Active continent–continent collision has taken place from Early Devonian to Mid-Carboniferous times (390–330 Ma), followed by post-thickening extension from the Mid-Carboniferous to the Permian (330–280 Ma). These events induced the development and tightening of arcuate structures like the Ibero–Armorican arc.

The internal domain of the Iberian segment constitutes the Central Iberian Zone (CIZ) according to the zonal division of Lotze (1945), modified by Julivert et al. (1974). In the CIZ three main ductile Hercynian deformation phases were recognized (Ribeiro, 1974; Noronha et al., 1979; Ribeiro et al., 1983; Diez Balda et al., 1990; Ribeiro et al., 1990a,b; Pereira et al., 1993). The probably continuous early Hercynian D1 and D2 phases are timed in the Mid-Upper Devonian (380–360 Ma) and Early to Mid-Carboniferous (360–330 Ma), respectively. They are characterized by the generation of subvertical D1 folds with a steep slaty cleavage and D2 recumbent folds with axial plane crenulation cleavage or schistosity associated with nappe emplacement. The D1 and D2 deformation phases correspond to the collisional stage of the Hercynian orogeny. This crustal thickening is associated with partial melting and a restricted production of peraluminous granitoids.

The last ductile deformation phase (D3), Namurian–Westphalian in age, develops open to tight vertical folds with subhorizontal axes and subvertical shear zones with a sinistral or dextral wrench movement. This ductile phase is followed by a fragile deformation phase (D4) in the Permian, giving rise to NE–SW, NNE–SSW and NW–SE fracture systems (Pereira et al., 1993). The D3 + D4 deformation is related to the post-thickening extension tectonics which follows the continent–continent collision and takes place from Mid-Carboniferous to Permian times. At the same time most of the CIZ

granitoids were emplaced defining alignments closely related to the ductile shear zones (Iglesias and Ribeiro, 1981; Ferreira et al., 1987a). They are characterized by highly contrasted compositions, from aluminopotassic to calc-alkaline and subalkaline types.

Based on the emplacement ages relatively to the main Hercynian events, namely D3, the CIZ granitoid magmatism has been classified (Ferreira et al., 1987a) as: (1) syn-orogenic pre-D3; (2) syn-orogenic syn- to late-D3; (3) late- to post-orogenic (post-D3, syn-D4).

A significant amount of Rb–Sr and K–Ar geochronological data of granitoids from the CIZ are available (for a compilation of the majority of the available data see Pinto et al., 1987; Beetsma, 1995). However some of these 'ages' are discrepant and disagree with geological data. This fact, as well as the known limitations of Rb–Sr and K–Ar isotopic systems and the advantage of comparing data obtained by multi-isotopic methods, lead us to the development of a U–Pb zircon and monazite geochronologic study. The objectives of this study are: (i) to date granitic rocks clearly related to known structural events and (ii) to constrain the timing of the last regional ductile deformation phase (D3) and of the fragile deformation phase (D4) that followed. For this purpose we have selected thirteen syn- to post-D3 units, representing the post-collisional plutonism in the CIZ. The term 'post-collisional' is used in the broad sense of post-thickening extension (Lagarde et al., 1992; Pereira et al., 1993; Rey et al., 1997).

2. Geology and petrography

The granitic plutons referred in this study are located in the CIZ, Northern Portugal and their distribution is controlled by the Vigo–Régua ductile shear zone or by the late Hercynian fragile fracturation and faulting, namely the Gerês–Lovios fault (Fig. 1). Several granitic plutons were selected (based on their internal structures and field relations) so as to represent different emplacement periods relatively to the third Hercynian tectonic phase (Fig. 1): (1) syn-D3 biotite granitoids: Ucanha-Vilar, Lamego, Sameiro and Refoios do Lima plutons; (2) late-D3
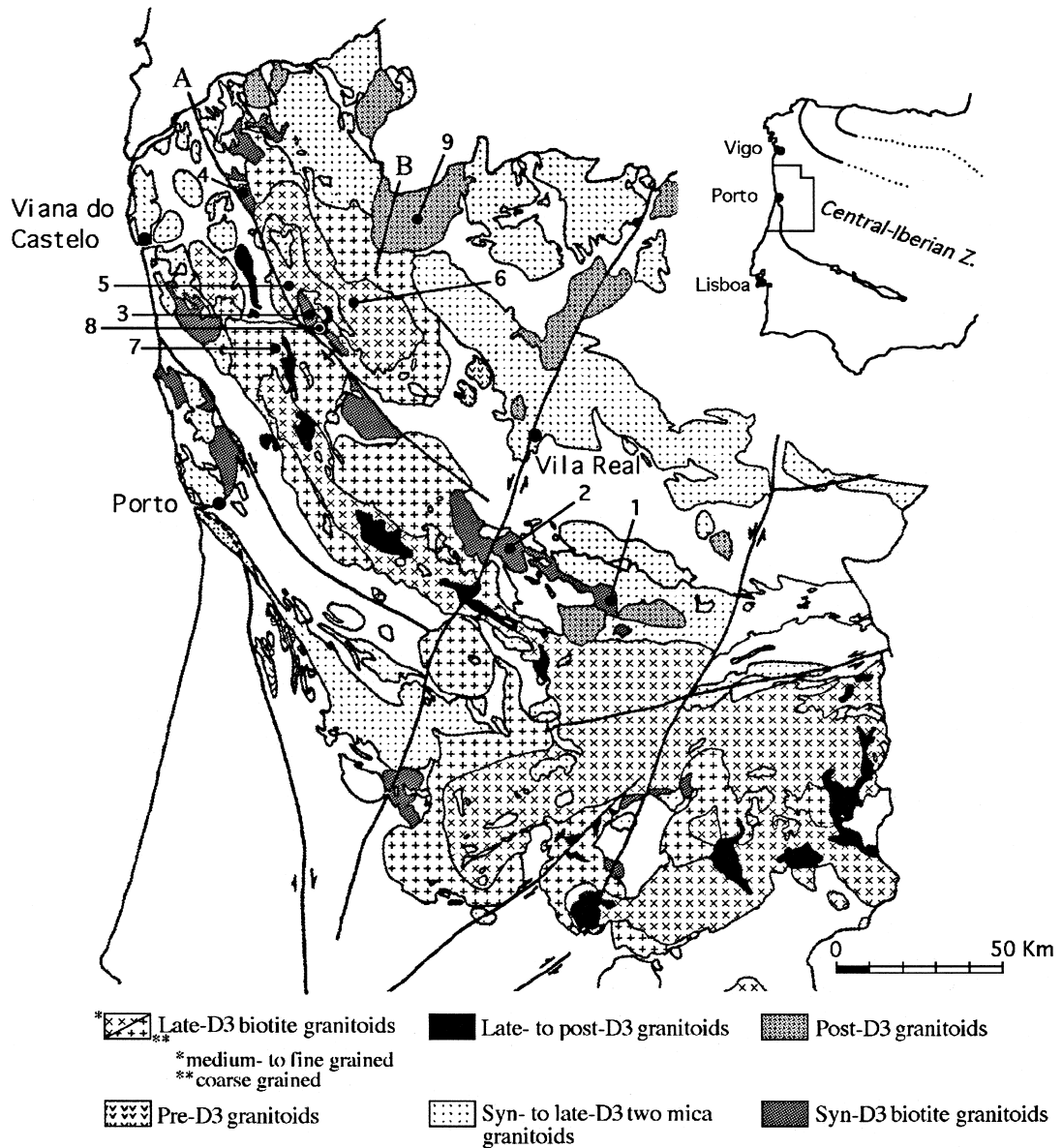
Fig. 1. Distribution of Hercynian syn- to post-orogenic granitoids in the Central Iberian Zone, Northern Portugal (Ferreira et al., 1987a, modified). (A) Vigo–Régua shear zone; (B) Gerês–Lovios fault. U–Pb dated plutons: *syn-D3 biotite granitoids* (1) Ucanha-Vilar, (2) Lamego, (3) Sameiro, (4) Refoios do Lima; *late-D3 biotite-dominant granitoids* (5) Braga pluton (Braga granite, associated basic to intermediate series and Gonça granite); (6) Agrela, (7) Celeirós; *late- to post-D3 granitoids* (8) Briteiros; *post-D3 granitoids* (9) Peneda–Gerês pluton (Gerês, Paufito, Illa and Carris granites); D3: last ductile deformation phase.

biotite-dominant granitoids: Braga (Braga granite, associated basic to intermediate series and Gonça granite), Agrela and Celeirós plutons; (3) late- to post-D3 granitoids: Briteiros granite; (4) post-D3 (syn-D4) granitoids: Peneda–Gerês pluton (Gerês, Paufito and Carris granites).

The main petrographic characteristics of the analysed samples from the different plutons are presented in Table 1.

2.1. Syn-D3 biotite granitoids

They include, among others and from south to north, the Ucanha-Vilar, Lamego, Sameiro and Refoios do Lima plutons. They are porphyritic (orthoclase phenocrysts) medium-grained biotite granodiorites–monzogranites and contain quartz + plagioclase (andesine/oligoclase) + perthitic orthoclase + iotite + zircon + monazite + apatite + ilmenite ± muscovite ± allanite (+cordierite + sillimanite in the Refoios do Lima pluton) (Simões et al., 1997a; Martins, 1997).

Microgranular enclaves occur dominantly in the Ucanha-Vilar, Lamego and Sameiro plutons and are rare in the Refoios do Lima pluton. A conspicuous planar fabric parallel to the Vigo–Régua shear zone is outlined by the alignment of orthoclase phenocrysts and biotite. They are considered early syn-D3 plutons, based on structural and geological features (Montenegro de Andrade et al., 1986; Pereira, 1992; Simões, in preparation).

2.2. Late-D3 biotite-dominant granitoids

This group is represented by the Braga, Agrela and Celeirós plutons (Ferreira et al., 1993). They present magmatic structures (preferential orientation of K-feldspar phenocrysts and partially of biotite) on conformity to D3.

The Braga massif is composite, associating two distinct granitic units (Dias and Leterrier, 1994): the Braga monzogranite which includes abundant microgranular enclaves and small stocks of gabbroic to granodioritic composition (gabbros, monzodiorites, quartz monzodiorites and granodiorites); the Gonça leucogranite which is devoid of mafic rocks and contains mica-rich enclaves and metasedimentary xenoliths. The Braga biotite monzogranite is slightly porphyritic, fine- to medium-grained and the biotite–muscovite Gonça leucogranite is fine-grained. The Agrela biotite monzogranite is porphyritic, medium-grained and includes abundant microgranular enclaves. This type of enclaves is rare in the

biotite-dominant Celeirós monzogranite which is porphyritic and coarse-grained (Dias et al., 1992).

The observed gradational contacts between the Braga–Gonça granites, Braga–Agrela granites and Agrela–Celeirós granites, as well as the sharp but lobated contacts between the Braga granite and the basic to intermediate bodies, indicate a synchronous emplacement of the different plutonic units.

The four granitic facies contain quartz, perthitic K-feldspar (orthoclase or microcline), plagioclase (oligoclase–andesine), biotite, muscovite (modal content 0–7%), ilmenite, apatite, zircon and monazite. Muscovite is an accessory phase in the Braga, Agrela and Celeirós granites. In the latter cordierite also occurs. Andalusite and sillimanite were observed in the Gonça granite. The quartz monzodiorite selected for U–Pb analysis contains orthoclase, andesine, quartz, Mg-rich biotite, Mg-rich actinolitic hornblende and accessory augite. Other minor phases are ilmenite, apatite, zircon and sphene.

2.3. Late- to post-D3 granitoids

These granitoids crosscut the plutons of groups (1) and (2) and their emplacement is controlled by late-Hercynian fracturation. They are represented in the Braga region by the Briteiros granite. Mica-rich enclaves are abundant in this two mica fine-grained leucogranite. It contains quartz, K-feldspar, plagioclase (albite–oligoclase), biotite, muscovite and the accessory mineralogy includes ilmenite, apatite, zircon, monazite, anatase and sillimanite.

2.4. Post-D3 granitoids

The Peneda–Gerês massif is a post-D3 pluton, whose emplacement is related with the fragile deformation phase D4. It is composed of four petrographic units, three of which are roughly concentric (Mendes, 1994; Mendes and Dias, 1996). The most extensive and external unit is the Gerês granite, a porphyritic coarse-grained biotite granite. It surrounds the Paufito granite, a porphyritic medium-grained biotite granite whose porphyritic character and grain-size decrease gradually towards the innermost unit, the Illa granite. This is a two mica medium- to fine-grained granite. The fourth unit, the Carris granite, is a porphyritic fine-grained biotite granite

Table 1
Mineralogical and geochemical characteristics of selected samples for zircon/monazite U–Pb analysis

	Syn-D3 granitoids				Late-D3 granitoids					Late- to post-D3 granitoid	Post-D3 granitoids			
Unit	Ucanha-Vilar	Lamego	Sameiro	Refoios do Lima	Braga massif			Agrela	Celeirós	Briteiros	Peneda–Gerês massif			
					Braga	Gonça	Qz-mzd				Gerês		Paufito	Carris
Sample	14B.3	14A.2	ST9.68	5A.2	PL9.88	ST9.85	B9.48	ST9.118	B9.74	ST9.67	G7	G63	M18	F9
Quartz	21.6	21.4	26.6	22.7	26.0	29.3	9.0	26.7	25.6	32.7	33.9	32.5	29.0	31.2
Plagioclase	40.0	41.4	35.7	38.3	33.8	27.3	39.8	34.4	29.7	24.0	33.9	34.5	36.1	35.3
	Olig–And	Olig–And	Olig–And	Olig–And	Olig–And	Olig–And	And	Olig–And	Olig–And	Ab–Olig	Ab–Olig	Ab–Olig	Ab–And	Ab–Olig
K-feldspar	21.7	15.6	18.1	10.1	24.1	28.7	11.1	23.3	28.6	23.3	25.4	25.8	26.0	27.5
Muscovite	0.5	0.7	1.3	5.5	1.3	7.4	–	1.5	1.0	12.1	0.9	1.3	0.8	0.7
Biotite	14.8	19.6	17.3	21.8	13.0	6.3	20.3	12.6	14.2	7.2	5.5	5.5	7.3	4.9
Amphibole	–	–	–	–	–	–	16.2	–	–	–	–	–	–	–
Cpx	–	–	–	–	–	–	1.5	–	–	–	–	–	–	–
Other	1.5	1.5	1.1	1.6	1.8	1.0	2.0	1.5	1.0	0.8	0.4	0.4	0.8	0.4
SiO_2 (%)	65.04	62.96	66.95	62.25	66.34	70.37	54.95	68.40	68.00	72.06	74.80	71.15	71.43	73.49
MgO (%)	1.47	1.87	1.22	1.85	1.14	0.48	5.16	1.08	0.93	0.48	0.27	0.27	0.63	0.29
Zr (ppm)	201	253	261	300	251	158	364	245	299	114	164	155	167	138
$(La/Yb)_N$	59.4	50.1	34.6	46.7	22.8	51.8	24.9	24.4	27.1	34.3	6.5	4.7	7.9	8.4

The norms (%) are estimated from the whole-rock and mineral chemical compositions. $(La/Yb)_N$ = La/Yb normalized ratios (normalization values from Evensen et al., 1978). Qz-mzd = quartz monzodiorite from the basic series. Ab = albite; Olig = oligoclase; And = andesine; Cpx = clinopyroxene.

that occurs as irregular masses in the Gerês granite. Contacts are gradational between the Paufito and Illa granites and sharp but lobated between the Gerês granite and the Paufito and Carris granites, therefore suggesting a sub-synchronous emplacement of all granites.

All four granitic units contain perthitic K-feldspar (dominantly orthoclase in the Gerês granite), plagioclase (albite–oligoclase, more rarely andesine), quartz, biotite, ilmenite, zircon and apatite. Certain minor phases are exclusive of some units, namely allanite in the Gerês granite, primary muscovite in the Illa granite and magnetite in the Carris granite. Other accessory minerals were observed, such as uraninite and thorite in the Paufito and Gerês granites and xenotime in the Gerês granite. Primary sphene, hornblende and monazite were found in some marginal areas of the Gerês granite.

3. Geochemistry

In previous studies whole-rock and mineral chemical data were obtained for the U–Pb dated units. The whole-rock compositions were determined at the CRPG (Nancy, France) by ICP–AES for the major and minor elements and by ICP–MS for the trace elements (including rare-earth elements) (Govindaraju and Mevelle, 1987). The estimated uncertainty of whole-rock analyses is 0.5% for major elements and 5–10% for trace elements.

Some relevant whole-rock chemical compositions of the U–Pb dated samples are presented in Table 1. Variation diagrams of selected major and trace elements are presented in Fig. 2 with parameter Fe + Mg + Ti (calculated in milliatom-grams of element per 100 g of rock and proportional to its mafic mineral content) as the differentiation index. Fig. 3 shows the chondrite-normalized REE patterns of the samples chosen for U–Pb dating. These samples are, in general, the least or one of the less evolved samples of the respective unit. The granitic typology indicated for each granite was based on mineralogical (biotite composition, Nachit et al., 1985; Rossi and Chevremont, 1987; zircon typology, Pupin, 1981, 1988) and chemical–mineralogical criteria (La Roche et al., 1980; Debon and Le Fort, 1983).

3.1. Syn-D3 biotite granitoids

The syn-D3 granitoids included in this study are moderately peraluminous granodiorites to monzogranites $[0 < Al − (K + Na + 2Ca) < 45$; Debon and Le Fort, 1983] of calc-alkaline to aluminopotassic affinity, except for the Refoios do Lima granite that exhibits typical aluminopotassic characteristics (Fig. 2; Simões et al., 1997b). They range from 62 to 70% SiO_2. Both mineral and whole-rock data show that all four plutons define separate evolutionary trends. The whole-rock chemical evolutions are characterized by a decrease in Si, Al, Ca, P, Ba, Sr, Zr and La with the decrease of parameter Fe + Mg + Ti. The Sameiro pluton is an exception and does not show significant chemical evolution. Noteworthy characteristics of these granitoids are the rather high Ba content (720–2181 ppm), high LREE enrichment $[(La/Yb)_N = 25–67]$ and moderate negative Eu anomalies (Eu/Eu∗ = 0.52–0.72) (Table 1, Figs. 2 and 3; Simões et al., 1997a).

3.2. Late-D3 biotite-dominant granitoids

The three units of the Braga massif (Braga granite, Gonça granite and basic to intermediate series) display a wide compositional range from gabbroic to granitic ($SiO_2 = 48.5–71\%$; MgO = 10.8–0.6%) and a subalkaline (monzonitic) affinity. The basic to intermediate series is dominantly metaluminous, the Braga granite reveals a slightly peraluminous character and the Gonça granite is typically peraluminous $[−102 < Al − (K + Na + 2Ca) < 52]$ (Fig. 2). On bivariate plots as Fig. 2 the three units define regular curves in which, with the decrease of Fe + Mg + Ti, the elements Si, K and Rb show an incompatible behaviour, Ca and Sr are compatible, whereas Ti, Ba, Zr, Y and REE show a two-step evolution from an incompatible to a compatible behaviour. Of the two granitic units, the Gonça leucogranite presents lower content of incompatible elements such as Ti, Zr, Y and HREE and steeper REE patterns $[(La/Yb)_N: 33–66]$ (Table 1, Fig. 3). The regular curve distribution suggests that the different units can be genetically related. In fact, Sr–Nd isotopic data are conformable with this massif being the result of an AFC process between a mantle-derived
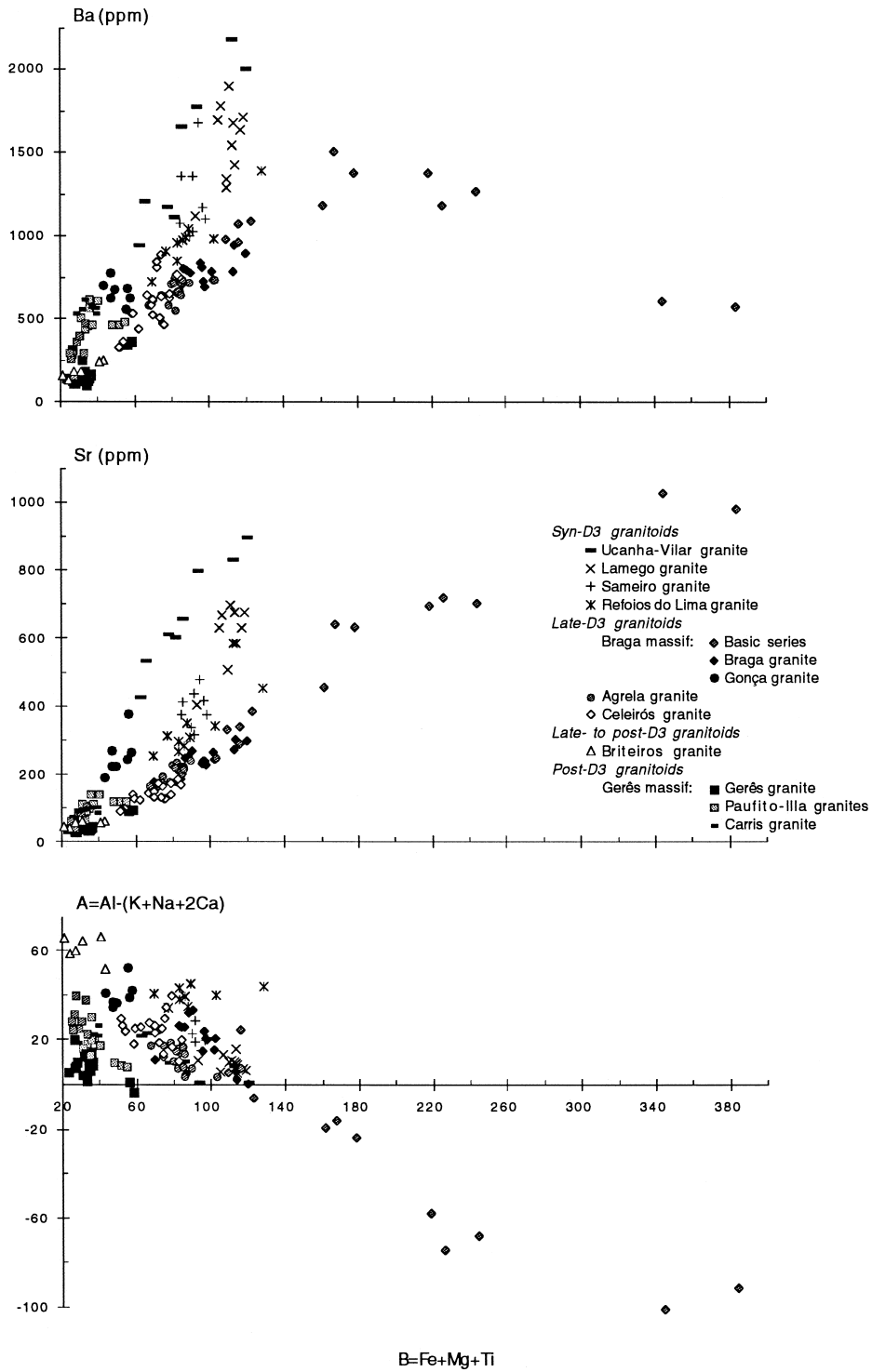
Fig. 2. Variation diagrams of Ba, Sr and A vs. B for the studied granitoids (chemical–mineralogical parameters A and B are in millications; B is proportional to the mafic content of the rock; Debon and Le Fort, 1983).
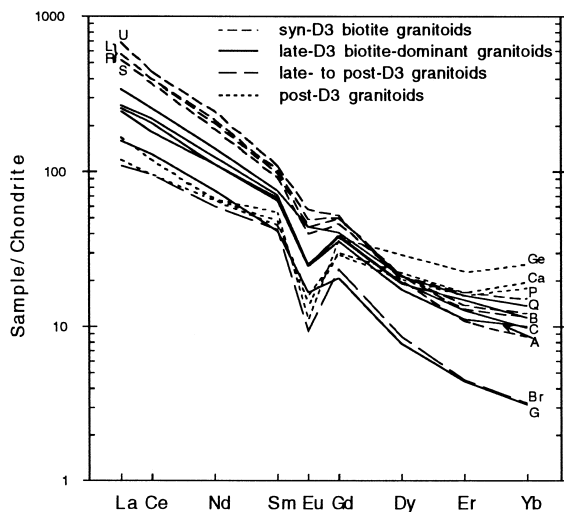
Fig. 3. Chondrite-normalized REE patterns of the U–Pb dated samples (REE normalization values are those of Evensen et al. (1978) for C1 chondrites). *Syn-D3 biotite granitoids*: (U) Ucanha-Vilar, (L) Lamego, (S) Sameiro, (R) Refoios do Lima; *late-D3 biotite-dominant granitoids*: (Q) quartz monzodiorite, (B) Braga, (G) Gonça, (A) Agrela, (C) Celeirós; *late- to post-D3 granitoids*: (Br) Briteiros; *post-D3 granitoids*: (G) Gerês, (P) Paufito, (C) Carris; D3: last ductile deformation phase.

magma (equivalent to the gabbroic term) and a crust-derived magma (the Gonça granite) (Dias and Leterrier, 1994).

The Agrela granite is identical to the Braga granite in both chemical (Figs. 2 and 3) and isotopic composition (Dias and Leterrier, 1993). The geochemical data indicate that these granites have no compositional relation with the Celeirós granite. This granitoid is slightly peraluminous $[10 < Al - (K + Na + 2Ca) < 34]$ with an aluminopotassic affinity (Fig. 2). A large and well defined internal chemical–mineralogical evolution is observed in this granite. With the decrease of parameter $Fe + Mg + Ti$, Si increases and Al, Ca, Ba, Sr, Zr, Y, REE decrease (Dias et al., 1992).

3.3. Late- to post-D3 granitoids

The two-mica Briteiros granite is an evolved peraluminous granite $[51 < Al - (K + Na + 2Ca) < 66]$ with an aluminopotassic affinity (Fig. 2). The SiO_2 content ranges between 70 and 73%. It presents steep REE patterns $[(La/Yb)_N = 14-35]$ and the total REE

concentrations are lower than in the other granites $(\Sigma REE = 58-133$ ppm) (Fig. 3). A discrete internal compositional evolution is observed, marked by the increase in Si and Rb and decrease in Al, Ca, Ba, Sr, Zr, REE with the decrease in mafic content (Dias et al., 1992).

3.4. Post-D3 granitoids

The four units that constitute the post-D3 Peneda–Gerês massif are slightly metaluminous to peraluminous monzogranites $[-4 < Al - (K + Na + 2Ca) < 40]$ of subalkaline ferro-potassic affinity (Fig. 2) (Mendes and Dias, 1996). Collectively they have evolved compositions (Fig. 2) with SiO_2 contents that are notably high in the Gerês granite (74–76.5%, with the exception of two samples with 71–72%) and range from 71 to 73% in the Paufito granite, 73–75% in the Illa granite and 73–74% in the Carris granite. These granites present comparatively less steep REE patterns $[(La/Yb)_N = 2.3-11.6;$ $(La/Sm)_N = 1.6-3.7]$, higher HREE content (13.8–41.9) and significant negative Eu anomalies $(Eu/Eu* < 0.5)$ (Fig. 3). The geochemical data indicate that the Gerês granite has no compositional relation with the other three units, whereas the two innermost units (Paufito and Illa granites) show a compositional and evolutionary continuity with the Paufito granite as the most primitive term. The Carris granite is compositionally identical to the Paufito granite (Fig. 1) and probably represents batches of the same magma surrounded by the magma that originated the Gerês granite. Internal chemical–mineralogical evolutions are observed in the Gerês and Paufito–Illa granites. With the decrease of the parameter $Fe + Mg + Ti$, SiO_2 increases and ΣREE, La/Yb, Zr and Th decrease. Additionally, in the Paufito–Illa series there is a decrease of Ca, Ba and Sr and an increase in K, Rb and negative Eu anomaly.

4. U–Pb geochronology

4.1. Analytical methods

Conventional U–Pb analysis of multi-grain zircon and/or monazite fractions (30 to 100 grains) were

carried out on a total of 14 samples from a quartz monzodiorite and granitic rocks. After crushing, minerals were separated using heavy liquids, magnetic separation and handpicking. For each sample three or four non-magnetic zircon fractions and one monazite fraction (when occurring) were selected, except for two samples where only a monazite fraction was selected. The handpicked grains were limpid, free of opaque inclusions and fractures. The selection of zircon fractions was based on size, morphology and colour. Some of these fractions were abraded as described by Krogh (1982) to minimize the effects of Pb loss. Polished epoxy mounts of fractions similar to those analysed were observed by backscattered scanning electron microscopy (BSEM).

The chemical separation of U and Pb was performed using methods adapted from Krogh (1973) and Parrish et al. (1987) and included: HNO_3 3 N washing; $HF + HNO_3$ digestion at 240°C and HCl 3 N dissolution of fluorides at 180°C in bomb; elution on anionic resin of two aliquots (one with addition of a mixed $^{235}U–^{208}Pb$ spike). Common lead blanks varied from 26 to 94 pg during this study. Isotopic measurements were done with a Cameca TSN 206 and a Finnigan MAT 262 mass spectrometers. The mass fractionation was estimated by systematic analysis of NBS 983 standard. Common lead corrections combine measured blanks and model of lead evolution of Stacey and Kramers (1975). Discordia line intercepts and associated errors (2σ) were calculated using the Isoplot program (Ludwig, 1987) in a simplified Macintosh version (Nemchin et al., 1994). All age determinations were calculated using the decay constants recommended by the IUGS Subcommission on Geochronology (Steiger and Jäger, 1977).

4.2. Results

For each granitoid group a description of zircon and monazite fractions in terms of shape, colour and internal structure is presented, followed by the age data. Isotopic data are listed in Table 2 together with the main zircon subtypes (Pupin, 1980) in each sample, when such information is available. The ages have been calculated considering the analytical uncertainties except in the case of the Sameiro and Carris granites, whose zircon fractions define reverse discordia, and for the Lamego granite, which has a very unprecise zircon fraction. For these three granites errors of 1% and a correlation coefficient of 0.98 were used. Data ages were plotted on conventional U–Pb concordia diagrams (Figs. 4–6). As will be evidenced further in the text, zircon and subconcordant monazite fractions from the same sample yield similar ages. Moreover, a good concordance exists between zircon and zircon + monazite ages, the latter yielding greater age precision. For these reasons, age results presented in Figs. 4–6 were calculated associating both mineral fractions in the cases where both minerals of a sample were analysed.

4.2.1. Syn-D3 biotite granitoids

For the U–Pb isotope analysis of the syn-D3 plutons one sample of each granitoid was selected. The zircon fractions were selected according to the morphology and length/width ratio of the zircons. All the zircons were transparent and colourless or slightly yellow. Different habits have been recognized: spherical (multifaceted diamond shape) (50–100 μm), short prismatic (100–150 μm), long prismatic (150–200 μm) to acicular (> 200 μm), lamellar (100–150 μm) and flat prismatic (ca. 150 μm). With the exception of the long prismatic to acicular zircons, all the fractions were subjected to air abrasion. BSEM imaging of the zircons show typical magmatic internal structures with zoning and nebulitic textures. Some zircons have internal structures with rounded pyramidal terminations, indicating different growth stages during magmatic crystallization. In the Sameiro granite, zircons with relict cores were observed.

According to their typological distribution (Pupin, 1980), the zircons of the selected granites are dominantly of subtypes S2, S3, S7 and S8 for the Ucanha-Vilar granite, S3, S7, S8 and S18 for the Lamego granite, S8, S12 and S13 for the Sameiro granite, and S7, S11 and S12 for the Refoios do Lima granite. They show typological evolutionary trends (Pupin, 1988) that indicate a calc-alkaline nature for the Ucanha-Vilar, Lamego and Sameiro granites, and a crustal or dominantly crustal origin for the Refoios do Lima granite (Simões et al., 1997b).

Table 2

U–Pb isotopic data on zircon and monazite from syn- to post-D3 Hercynian granitoids (Northern Portugal)

Granitoid (dominant zircon subtypes)	Fraction (crystal habit)	Weight (mg)	U (ppm)	Pb* (ppm)	^{206}Pb/^{204}Pb (2σ)	^{206}Pb*/^{238}U (2σ, %)	^{207}Pb*/^{235}U (2σ, %)	^{207}Pb*/^{206}Pb* (2σ, %)	Age (Ma) ^{206}Pb*/^{238}U (2σ)	Age (Ma) ^{207}Pb*/^{235}U (2σ)	Age (Ma) ^{207}Pb*/^{206}Pb* (2σ)
Syn-D3 granitoids											
Ucanha-Vilar (S2, S3, S7, S8)	14B.3/A (Z) (long p.)	0.73	1975.4	90.2	1828 (11)	0.04756 (0.12)	0.34546 (0.31)	0.05268 (0.20)	299.5 (0.3)	301.3 (0.8)	315 (3)
	14B.3/B (Z) (short p.)	0.65	1915.5	89.3	1907 (12)	0.04793 (0.11)	0.34824 (0.33)	0.05269 (0.24)	301.8 (0.3)	303.4 (0.9)	316 (4)
	14B.3/C (Z) (lamellar)	0.87	2139.5	95.7	1822 (13)	0.04645 (0.10)	0.33737 (0.31)	0.05267 (0.22)	292.7 (0.3)	295.2 (0.8)	315 (3)
	14B.3/D (Z) (acicular)	0.18	2248.1	91.5	1437 (9)	0.04265 (0.09)	0.30986 (0.33)	0.05269 (0.25)	269.3 (0.2)	274.1 (0.8)	315 (6)
	14B.3 (Mz)	1.15	1515.3	664.7	4235 (8)	0.05047 (0.79)	0.36616 (0.89)	0.05262 (0.10)	317.4 (2.5)	316.8 (2.4)	312 (3)
Lamego (S3, S7, S8, S18)	14A.2/A (Z) (long p.)	0.07	1366.5	45.1	1167 (3)	0.03091 (0.33)	0.22486 (0.47)	0.05276 (0.15)	196.3 (0.6)	205.9 (0.9)	318 (2)
	14A.2/B (Z) (flat p.)	0.37	962.2	43.5	2763 (23)	0.04585 (0.19)	0.33319 (1.57)	0.05271 (1.39)	289.0 (0.5)	292.0 (4.0)	316 (27)
	14A.2/C (Z) (spherical)	0.27	919.5	45.0	1715 (5)	0.05020 (0.07)	0.36558 (0.23)	0.05282 (0.16)	315.7 (0.2)	316.4 (0.6)	321 (3)
Sameiro (S8, S12, S13)	ST9.68/B (Z) (short p.)	0.13	685.5	41.4	3208 (8)	0.05643 (0.20)	0.47863 (0.29)	0.06152 (0.09)	353.9 (0.7)	397.1 (0.9)	657 (1)
	ST9.68/C (Z) (spherical)	0.30	1107.9	60.9	4013 (4)	0.05449 (0.06)	0.44506 (0.14)	0.05924 (0.09)	342.0 (0.2)	373.8 (0.5)	576 (2)
	ST9.68/D (Z) (long p.)	0.09	947.5	46.9	1544 (2)	0.05043 (0.06)	0.37188 (0.20)	0.05349 (0.15)	317.1 (0.2)	321.0 (0.6)	349 (3)
	ST9.68 (Mz)	0.56	2714.0	553.6	3688 (8)	0.05055 (0.73)	0.36708 (0.85)	0.05266 (0.12)	317.9 (2.3)	317.5 (2.3)	314 (3)
Refoios do Lima (S7, S12, S11)	5A.2/A (Z) (acicular)	0.19	717.4	36.0	1989 (8)	0.04541 (0.24)	0.33032 (0.50)	0.05275 (0.27)	286.3 (0.7)	289.8 (1.3)	318 (4)
	5A.2/B (Z) (long p.)	0.20	814.6	37.3	2090 (13)	0.04514 (0.10)	0.32819 (0.36)	0.05273 (0.27)	284.6 (0.3)	288.2 (0.9)	318 (5)
	5A.2/E (Z) (short p.)	0.15	808.0	36.8	1438 (2)	0.04708 (0.05)	0.34244 (0.17)	0.05275 (0.12)	296.6 (0.2)	299.0 (0.4)	318 (3)
	5A.2 (Mz)	0.48	4353.9	822.2	6596 (13)	0.05057 (0.87)	0.36700 (0.97)	0.05264 (0.10)	318.0 (2.7)	317.4 (2.7)	313 (2)
Late-D3 granitoids											
Braga	PL9.88/1 (Z) (spherical)	0.10	692.6	35.7	982 (1)	0.04346 (0.19)	0.31489 (0.49)	0.05255 (0.31)	274.2 (0.5)	278.0 (1.2)	309 (9)
	PL9.88/2 (Z) (long p.)	0.14	701.1	31.5	2106 (2)	0.04496 (0.13)	0.32619 (0.27)	0.05262 (0.13)	283.5 (0.4)	286.7 (0.7)	313 (4)

	PL9.88/3 (Z) (flat p.)	0.07	1172.9	50.7	2769 (3)	0.04346(0.17)	0.31500 (0.31)	0.05257 (0.14)	274.2 (0.4)	278.1 (0.8)	310 (3)
	PL9.88 (Mz)	0.12	3610.5	1282.8	2982 (8)	0.05126 (1.14)	0.37117 (1.29)	0.05252 (0.15)	322.2 (3.6)	320.5 (3.5)	308 (4)
Quartz monzodiorite	B9.48/1 (Z) (spherical)	0.29	1283.3	61.5	2215 (2)	0.04424 (0.27)	0.32030 (0.37)	0.05251 (0.10)	279.1 (0.7)	282.1 (0.9)	307 (4)
	B9.48/2 (Z) (fragments)	0.58	685.3	39.1	6219 (5)	0.04597 (0.14)	0.33309 (0.23)	0.05255 (0.09)	289.7 (0.4)	291.9 (0.6)	310 (2)
	B9.48/3 (Z) (fragments)	0.18	464.2	28.3	1125 (2)	0.04832 (0.17)	0.35002 (0.37)	0.05253 (0.21)	304.2 (0.5)	304.7 (1.0)	309 (4)
Gonça	ST9.85/1 (Z) (spherical)	0.14	496.5	25.3	703 (2)	0.05213 (0.13)	0.43164 (0.34)	0.06005 (0.23)	327.6 (0.4)	364.3 (1.1)	605 (8)
	ST9.85/2 (Z) (long p.)	0.02	1919.5	81.4	426 (0.5)	0.04319 (0.11)	0.31278 (0.39)	0.05253 (0.30)	272.6 (0.3)	276.3 (0.9)	308 (7)
	ST9.85/3 (Z) (flat p.)	0.03	2909.2	123.9	399 (1)	0.04489 (0.35)	0.32524 (0.70)	0.05255 (0.38)	283.1 (1.0)	285.9 (1.7)	309 (11)
	ST9.85/4 (Z) (short p.)	0.07	1066.9	48.2	1054 (3)	0.04644 (0.08)	0.33660 (0.22)	0.05257 (0.15)	292.6 (0.2)	294.6 (0.6)	310 (3)
	ST9.85 (Mz)	0.28	5578.2	1306.0	6359 (19)	0.05021 (2.93)	0.36375 (3.10)	0.05254 (0.18)	315.8 (9.0)	315 (8.4)	309 (4)
Agrela	ST9.118/1 (Z) (spherical)	0.21	740.1	40.4	2928 (8)	0.05465 (0.20)	0.43567 (0.36)	0.05782 (0.16)	343.0 (0.7)	367.2 (1.1)	525 (4)
	ST9.118/2 (Z) (long p.)	0.04	2106.3	90.7	891 (2)	0.04423 (0.09)	0.31988 (0.30)	0.05245 (0.21)	279.0 (0.3)	281.8 (0.7)	305 (5)
	ST9.118/3 (Z) (flat p.)	0.08	1380.3	55.0	1206 (8)	0.04165 (0.19)	0.30068 (0.49)	0.05236 (0.33)	263.1 (0.5)	266.9 (1.2)	304 (8)
	ST9.118/4 (Z) (short p.)	0.14	786.2	38.7	764 (0.6)	0.04822 (0.14)	0.34914 (0.31)	0.05252 (0.17)	303.6 (0.4)	304.1 (0.8)	308 (4)
	ST9.118 (Mz)	0.12	4084.3	1483.6	3764 (19)	0.04978 (1.66)	0.36016 (1.85)	0.05247 (0.19)	313.2 (5.1)	312.3 (5.0)	306 (4)
Celeirós	B9.74/1 (Z) (spherical)	0.26	584.8	28.4	3464 (8)	0.04929 (0.10)	0.38966 (0.22)	0.05734 (0.12)	310.2 (0.3)	334.1 (1.0)	504 (4)
	B9.74/2 (Z) (long p.)	0.10	892.9	40.2	1811 (2)	0.04599 (0.10)	0.33291 (0.27)	0.05250 (0.17)	289.9 (0.3)	291.8 (0.7)	307 (4)
	B9.74/3 (Z) (flat p.)	0.16	847.4	39.6	1377 (2)	0.04427 (0.19)	0.32048 (0.38)	0.05250 (0.19)	279.2 (0.5)	282.3 (0.9)	310 (7)
	B9.74/4 (Z) (short p.)	0.03	1847.3	83.2	633 (0.7)	0.04584 (0.15)	0.33174 (0.40)	0.05249 (0.26)	288.9 (0.4)	290.9 (1.0)	307 (5)
	B9.74 (Mz)	0.36	2983.2	1141.0	4721 (13)	0.05082 (1.49)	0.36763 (1.62)	0.05247 (0.13)	319.5 (4.6)	317.9 (4.4)	306 (4)

Table 2 (continued)

Granitoid (dominant zircon subtypes)	Fraction (crystal habit)	Weight (mg)	U (ppm)	Pb* (ppm)	$^{206}Pb/^{204}Pb$ (2σ)	$^{206}Pb*/^{238}U$ (2σ, %)	$^{207}Pb*/^{235}U$ (2σ, %)	$^{207}Pb*/^{206}Pb*$ (2σ, %)	Age (Ma) $^{206}Pb*/^{238}U$ (2σ)	Age (Ma) $^{207}Pb*/^{235}U$ (2σ)	Age (Ma) $^{207}Pb*/^{206}Pb*$ (2σ)
Late- to post-D3 granitoids											
Briteiros	ST9.67 (Mz)	0.06	5696.6	683.8	3357 (12)	0.04756 (0.29)	0.34374 (0.42)	0.05242 (0.13)	299.5 (0.9)	300.0 (1.1)	304 (3)
Post-D3 granitoids											
Paufito (S25, S20, S15)	M18.tr.1 (Z) (short p.)	0.65	963.4	41.2	4484 (15)	0.04405 (0.68)	0.31654 (0.78)	0.05212 (0.10)	277.9 (1.9)	280.0 (1.9)	291 (2)
	M18.tr.2 (Z) (short p.)	0.11	1856.6	75.9	2762 (9)	0.03743 (0.11)	0.26944 (0.25)	0.05221 (0.15)	236.9 (0.2)	242.2 (0.5)	294 (3)
	M18.tr.3 (Z) (short p.)	0.24	1106.8	48.2	678 (0.7)	0.04373 (0.09)	0.31442 (0.24)	0.05215 (0.16)	275.9 (0.2)	277.6 (0.6)	292 (4)
	M18.pr (Z) (long p.)	0.07	2094.7	84.0	778 (2)	0.04110 (0.15)	0.29541 (0.37)	0.05213 (0.23)	259.6 (0.4)	262.8 (0.9)	291 (3)
Carris	F9.tr.1 (Z) (short p.)	0.33	1066.7	55.9	3604 (8)	0.05348 (0.44)	0.43003 (0.55)	0.05832 (0.11)	335.8 (1.5)	363.2 (1.7)	542 (3)
	F9.tr.2 (Z) (short p.)	0.15	848.4	44.0	1452 (5)	0.05251 (0.26)	0.41687 (0.43)	0.05758 (0.18)	329.9 (0.8)	353.8 (1.3)	515 (4)
	F9.pr (Z) (long p.)	0.09	1162.5	56.8	516 (0.8)	0.04649 (0.15)	0.34493 (0.43)	0.05381 (0.29)	292.9 (0.4)	300.9 (1.1)	363 (9)
	F9.tr.3 (Z) (short p.)	0.29	1984.4	96.2	1143 (0.8)	0.04936 (0.12)	0.3773 (0.25)	0.05544 (0.13)	310.6 (0.4)	325.1 (0.7)	430 (3)
Gerês (S25, S20, P3, P2)	G7.tr.1 (Z) (short p.)	0.11	1435.1	65.5	160 (0.1)	0.03866 (0.20)	0.27857 (0.70)	0.05225 (0.54)	244.5 (0.5)	249.5 (1.6)	297 (11)
	G7.tr.2 (Z) (short p.)	0.08	1703.3	82.9	1195 (1)	0.04170 (0.12)	0.30065 (0.25)	0.05228 (0.13)	263.4 (0.3)	266.9 (0.6)	298 (3)
	G7.pr (Z) (long p.)	0.17	1323.3	63.2	311 (0.2)	0.04015 (0.11)	0.28934 (0.45)	0.05227 (0.36)	253.7 (0.3)	258.0 (1.0)	297 (4)
	G7.tr.3 (Z) (short p.)	0.14	1724	77.4	926 (1)	0.04501 (0.11)	0.32432 (0.33)	0.05226 (0.23)	283.8 (0.3)	285.2 (0.8)	296 (3)
	G63 (Mz)	0.46	2432.1	672.1	5980 (47)	0.04701 (0.79)	0.33850 (0.95)	0.05222 (0.17)	296.1 (2.3)	296.0 (2.4)	295 (4)

Zircon sub-types after Pupin (1980). Uncertainties on calculated isotopic ratios (in %) are corrected for blanks and initial common Pb (Stacey and Kramers, 1975).
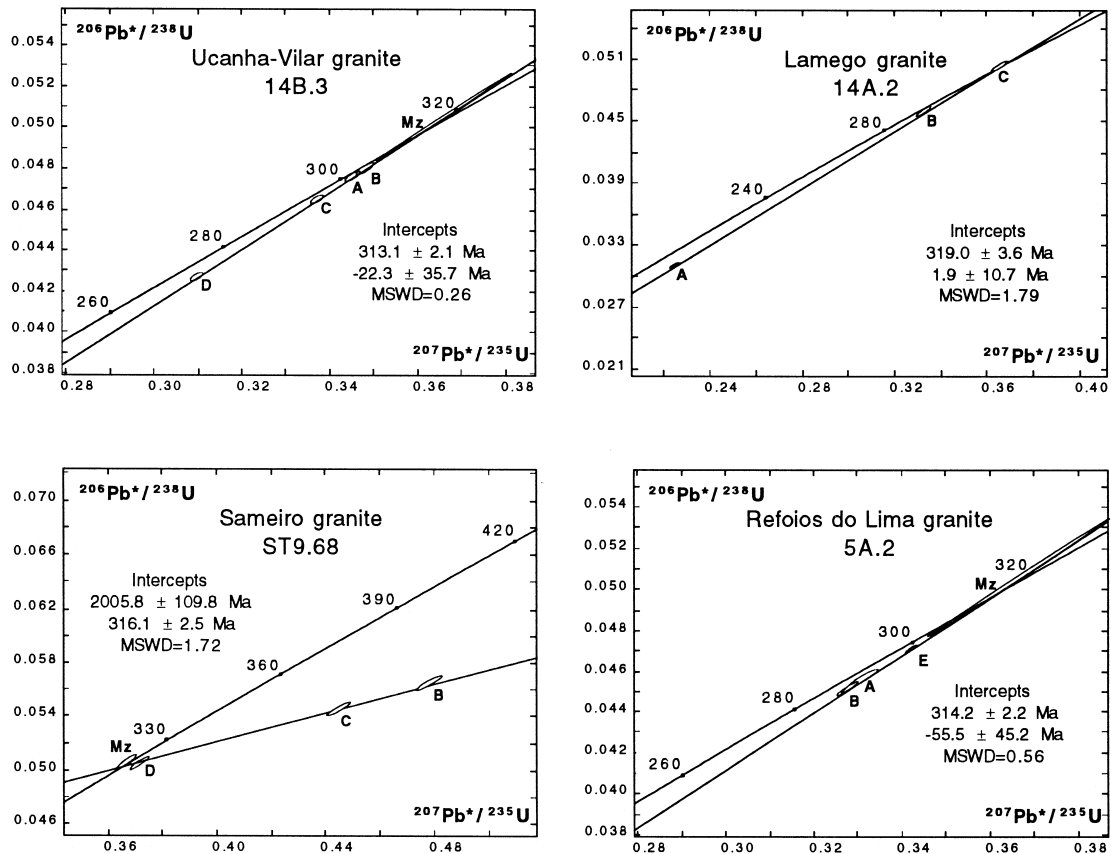Z = zircon; Mz = monazite; p = prismatic; Pb* = radiogenic lead.

Fig. 4. Conventional concordia diagrams for zircon and monazite fractions from syn-D3 biotite granitoids.

4.2.1.1. Ucanha-Vilar granite. Four zircon fractions and one monazite fraction were analysed. The monazite is slightly reversely discordant (−1.76% discordancy) giving a ^{207}Pb/^{235}U age of 317 ± 3 Ma. The four zircon fractions define a direct discordia (MSWD = 3.6) with an upper intercept at 315 ± 5 Ma. The good concordance of monazite and zircon ages enables us to associate the two minerals which define a good alignment (MSWD = 0.3) with an upper intercept at 313 ± 2 Ma (Fig. 4).

4.2.1.2. Lamego granite. Three zircon fractions were analysed and the data points define a normal discordia whose upper intercept with the concordia is at 319 ± 4 Ma (MSWD = 2.1) (Fig. 4). This age, well constrained by the ^{207}Pb/^{206}Pb age (321 ± 3 Ma) of the most concordant fraction (14A.2/C, 1.68% discordancy), can be considered as the crystallization age of the granite.

4.2.1.3. Sameiro granite. Three zircon fractions and one monazite fraction were analysed. The monazite fraction is slightly reversely disconcordant (−1.27% discordancy) with a ^{207}Pb/^{235}U age of 318 ± 2 Ma. The zircon fractions define a reverse discordia (MSWD = 8.3) with a lower intercept at 314 ± 4 Ma and an upper intercept at 1932 ± 126 Ma. All considered monazite and zircon fractions define a reverse discordia (MSWD = 1.7) with a lower intercept at 316 ± 2 Ma (upper intercept at 2006 ± 110 Ma), similar to the above monazite and zircon ages (Fig. 4). It may therefore be assumed as the emplacement age of the Sameiro granite. The reverse discordia is interpreted as indicating the existence of inherited lead, which is confirmed by the observation of inherited cores by BSEM imagery.

4.2.1.4. Refoios do Lima granite. Three zircon fractions and one monazite fraction were analysed. The
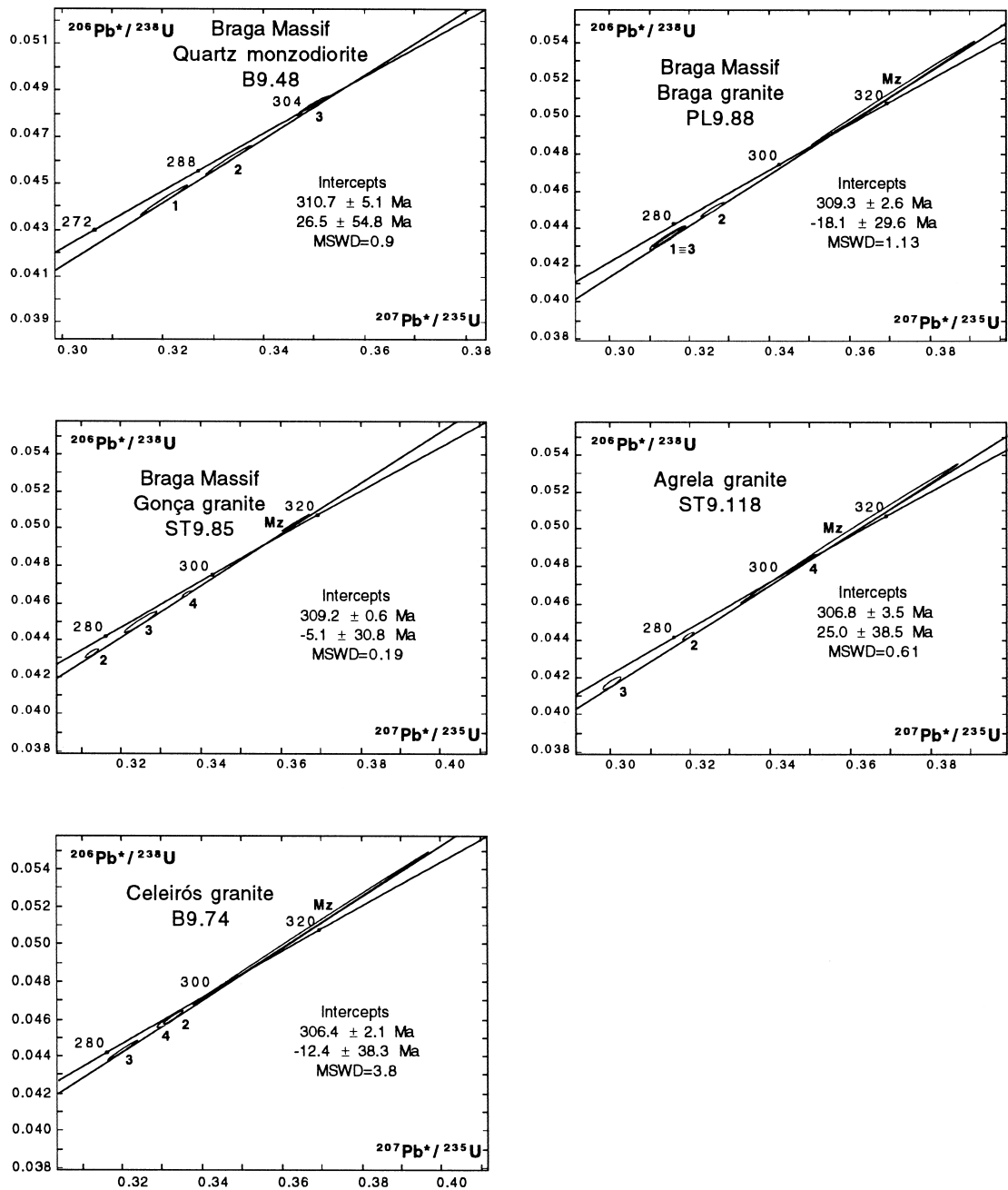
Fig. 5. Conventional concordia diagrams for zircon and monazite fractions from late-D3 biotite-dominant granitoids.

monazite fraction is almost concordant $(-1.62\%$ discordancy) yielding a $^{207}\text{Pb}/^{235}\text{U}$ age of 317 ± 3 Ma, whereas the zircon fractions define a poorly aligned normal discordia $(\text{MSWD} = 5.8)$ with an

upper intercept at 319 ± 13 Ma. Together, monazite and zircon fractions are well aligned along a normal discordia $(\text{MSWD} = 0.6)$ with an upper intercept at 314 ± 2 Ma (Fig. 4).
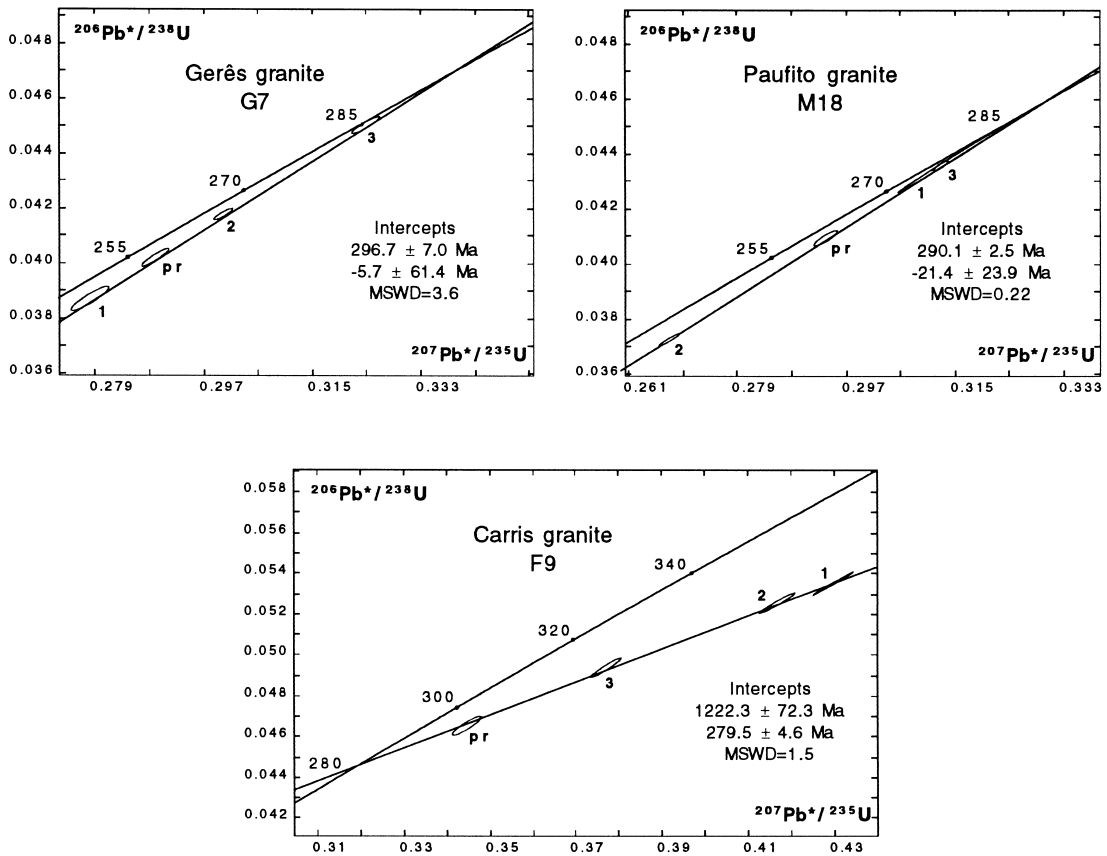
Fig. 6. Conventional concordia diagrams for zircon fractions from the post-D3 granitoids that constitute the Peneda–Gerês massif.

4.2.2. Late-D3 biotite-dominant granitoids

Three zircon fractions from the Braga granite (sample PL9.88) and four zircon fractions per sample from Gonça, Agrela and Celeirós granites (samples ST9.85, ST9.118 and B9.74, respectively) were analysed. Four different populations of zircon have been recognized in all granitic samples.

(i) Spherical, euhedral and multifaceted zircons. They are limpid, colourless to pale pink or yellow, being however less frequent in the Celeirós granite. Subhedral (sometimes partially corroded) to rounded cores are often recognized, surrounded by finely zoned rims.

(ii) Short prismatic zircons (1:2 to 1:3 shape ratios). They are abundant, transparent to slightly translucent, colourless or pale pink/yellow and often fractured. BSEM images show a clear growth discontinuity between a partially resorbed inner zone with a

nebulitic, faint zoning, and a finely zoned outer zone. These structures are interpreted as magmatic, probably developed in two crystallization steps and revealing some desequilibrium between the early generation and the liquid.

(iii) Long prismatic to acicular zircons (1:7 to 1:10 shape ratios). They are abundant, limpid and colourless, showing a regular fine magmatic zoning, more nebulitic in the centre of each crystal.

(iv) Flat prismatic zircons. They are not common, very limpid, colourless and sometimes corroded. BSEM images reveal homogenous crystals devoid of cores and show a faintly zoned dominantly nebulitic internal structure.

From the same granitic samples a total of four monazite fractions were separated. They are comprised of euhedral, short prismatic, limpid and pale yellow crystals.

In the quartz monzodiorite (sample B9.48) from the Braga massif two zircon populations have been recognized: (i) multifaceted and spherical, limpid and colourless to pale pink zircons; (ii) abundant fragments of prismatic and flat prismatic pink zircons, strongly fractured. In BSEM imagery all the observed grains are devoid of cores, unzoned or with a weakly zoned border mainly in population (ii). Sometimes a sector-zoned internal structure is observed in population (i).

It must be noted that the multifaceted spherical zircons from Gonça, Agrela and Celeirós granites are largely discordant with $^{207}Pb/^{206}Pb$ ages greater than 500 Ma. Such discordancy can be interpreted as reflecting the presence in these zircon fractions of inherited lead. This indicates that some of the cores observed by BSEM imagery are inherited. For this reason these fractions were not taken into account for the age calculations.

4.2.2.1. Braga massif. The three zircon fractions of each of the two granite units (Braga and Gonça granites) define poorly aligned normal discordias (MSWD = 3.6 and 8.5, respectively) with upper intercepts at 310 ± 15 Ma for the Braga granite and 312 ± 10 Ma for the Gonça granite. The monazite fractions of the Braga and Gonça granites are reversely discordant (-4.53 and -2.21% discordancy, respectively). For each unit the association of zircon and monazite fractions yield well aligned normal discordias whose upper intercepts with the concordia curve are: 309 ± 3 Ma (MSWD = 1.1) for the Braga granite and 309 ± 1 Ma (MSWD = 0.2) for the Gonça granite (Fig. 5).

The upper intercept of the normal discordia line that best fits all the quartz monzodiorite zircon fractions is at 311 ± 5 Ma (MSWD = 0.9) (Fig. 5). The fraction B9.48/3 (fragments of prismatic and flat prismatic pink zircons) provides a slightly normal discordancy (1.62%) and yields a $^{207}Pb/^{206}Pb$ age of 309 ± 4 Ma which comforts the discordia age.

4.2.2.2. Agrela granite. The zircon fractions define a normal discordia with an upper intercept at 309 ± 5 Ma (MSWD = 9.7). Although unprecise, this age is ensured by the $^{207}Pb/^{206}Pb$ age of 308 ± 4 Ma of the almost concordant (1.50% discordancy) short prismatic fraction (ST9.118/4). The monazite frac-

tion is reversely discordant (-2.35% discordancy). The zircon and monazite fractions reveal a good alignment (MSWD = 0.6), defining a normal discordia line that intercepts the concordia at 307 ± 3.5 Ma (upper intercept) (Fig. 5).

4.2.2.3. Celeirós granite. Zircon U–Pb data plot very close together and define a normal discordia whose upper intercept indicates the unprecise age of 307 ± 12 Ma (MSWD = 4.8). The monazite fraction is reversely discordant (-4.34% discordancy). Its association with the zircon fractions yields a better-fit normal discordia line (MSWD = 3.8) with an upper intercept at 306 ± 2 Ma (Fig. 5).

4.2.3. Late- to post-D3 granitoids

Due to the rarity of zircons in the Briteiros two-mica granite, only an euhedral round-shaped monazite fraction has been analysed. It is almost concordant (1.54% discordancy) and yields a $^{207}Pb/^{235}U$ age of 300 ± 1 Ma. This value is considered as the crystallization age of the granite and agrees with geological data for this granitoid group which cross-cuts the two previous syn- and late-D3 granitoids.

4.2.4. Post-D3 granitoids

U–Pb geochronology was undertaken for three of the four granites that constitute the Peneda–Gerês massif, the Paufito, Gerês and Carris granites. For each granite one sample was selected from which four zircon fractions per sample were obtained. For the Gerês granite an additional sample was used and one monazite fraction was obtained.

In all three granites the great majority of the good quality zircons had a short prismatic form (length/width ratio of 1.5–2), therefore only one of the four zircon fractions corresponds to long prismatic zircons. Some of the selected zircons were colourless and clear. Such was the case of the long prismatic fractions and the short prismatic fractions not subjected to air abrasion. The other short prismatic zircons had a very light yellow colour corresponding to a fine late overgrowth that was at least partially discarded during the air abrasion process. BSEM imaging showed that the zircons contained a zoned internal structure and that inherited cores were successfully avoided during handpicking, except in the case of the Carris granite where almost impercep-

tible inherited cores were present. The monazite fraction was comprised of yellow translucent grains and fragments.

The zircons of the analysed granites are dominantly of subtypes corresponding to the right-half of the zircon typological diagram (Pupin, 1980) and define typological evolutionary trends (Pupin, 1988) that are typical of subalkaline granites, going from subtypes S24, S25 to subtypes S4, S5, P1 and G1 (Mendes et al., 1997).

4.2.4.1. Gerês granite. The four zircon fractions (sample G7) scatter along a single chord (MSWD = 3.6) with an upper intercept of the concordia at 297 ± 7 Ma (Fig. 6). The analysed monazite fraction (sample G63) is almost concordant (−0.40% discordancy) and provided a $^{207}Pb/^{235}U$ age of 296 ± 2 Ma. This age, which is very close to the zircon age and more precise, can be accepted as the crystallization age of this granite.

4.2.4.2. Paufito granite. The four zircon data points define a normal discordia that intersects concordia at 290 ± 2.5 Ma (MSWD = 0.2) (Fig. 6). The less discordant fractions correspond to the clear short prism fraction (4.60% discordancy) and the overgrowth-bearing short prism fraction abraded during longer period of time (5.63% discordancy).

4.2.4.3. Carris granite. All four zircon fractions define a reverse discordia (MSWD = 1.5) that intersects concordia at 280 ± 5 Ma and 1222 ± 72 Ma (Fig. 6). The lower intercept age represents a minimum crystallization age for the granite whereas the upper intercept age reflects the age or ages of the inherited component. The existence of an inherited component was confirmed by BSEM observations that revealed a less evidence of inherited cores in the long prismatic zircons.

5. Discussion and conclusions

Four granitic plutons representing the Hercynian syn-D3 granitoid group were dated (Fig. 7). The monazite ages obtained for the Ucanha-Vilar, Sameiro and Refoios do Lima granites are identical (317 ± 3 Ma, 318 ± 2 Ma and 317 ± 3 Ma, respec-

tively) and close to the corresponding zircon ages (315 ± 5 Ma, 314 ± 4 Ma and 319 ± 13 Ma, respectively). The calculated U–Pb zircon or zircon + monazite ages are interpreted as crystallization ages: 313 ± 2 Ma for the Ucanha-Vilar pluton, 319 ± 4 Ma for the Lamego pluton, 316 ± 2 Ma for the Sameiro pluton and 314 ± 2 Ma for the Refoios do Lima pluton. Considering the uncertainties, the narrow range between 313 and 319 Ma can therefore be interpreted as representing an almost synchronous emplacement of the different plutons, early syn-D3, in agreement with geological data. This age range conforms with the Namurian/Westphalian age group (315 ± 3 Ma) of Pinto (1985), in a time scale proposed by the author for Portuguese granitoids, based on Rb–Sr and K–Ar isotopic data. K–Ar biotite ages are available for the Ucanha-Vilar pluton and are of 294 ± 6 Ma, 306 ± 6 Ma and 294 ± 5 Ma (Ferreira et al., 1987b). The discordance between U–Pb and K–Ar ages (8–20 Ma) suggests that this granite underwent cooling or reheating up to 294 Ma.

For the three units of the late-D3 Braga massif (Braga granite, associated quartz monzodiorite and Gonça granite) almost equivalent zircon ages were obtained (310 ± 15 Ma, 311 ± 5 Ma and 312 ± 10 Ma, respectively). Greater age precision is obtained for the Braga and Gonça granites when zircon and monazite fractions are associated: 309 ± 3 Ma for the Braga granite, 309 ± 1 Ma for the Gonça granite (Fig. 7). The very narrow range of 309–311 Ma is in agreement with geological interpretation (late-D3 emplacement) and with the coeval emplacement of the three units. These ages are concordant with the Rb–Sr whole-rock age of 310 ± 10 Ma (MSWD = 0.2) obtained for the Braga granite in a previous study (Dias and Leterrier, 1994).

The Agrela and Celeirós late-D3 granites have identical zircon (309 ± 5 Ma and 307 ± 12 Ma, respectively) and zircon + monazite U–Pb ages (307 ± 3.5 Ma and 306 ± 2 Ma, respectively) (Fig. 7), being the latter considered as the crystallization age of these granitoids. In a previous study Dias and Leterrier (1993) obtained Rb–Sr whole-rock ages of 307 ± 10 Ma (MSWD = 2.2) for the Agrela granite and 308 ± 6 Ma (MSWD = 0.7) for the Celeirós granite. These values agree with the new U–Pb determinations which are more precise and in accordance with the proposed synchronous emplacement
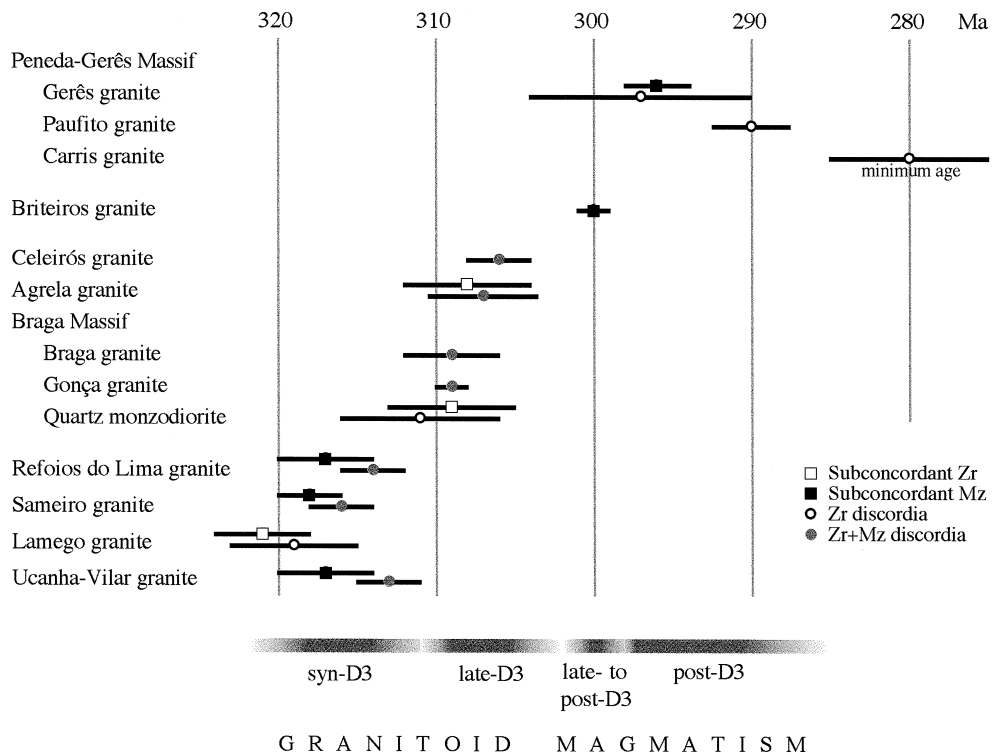
Fig. 7. Summary of U–Pb zircon/monazite data of syn- to post-D3 Hercynian granitoids (CIZ, Northern Portugal).

of both units. The above U–Pb ages are not significantly younger than the Braga massif age, when considering the analytical errors (Fig. 7). In fact these three plutons are spatially associated and are considered coeval. Consequently, the age range of about 306–311 Ma can be considered as the age of the late-D3 plutonism in the studied area.

The late- to post-D3 plutonic event is marked by the emplacement of the Briteiros granite which crosscuts granitoids from the two previous groups. The crystallization age of monazite at 300 ± 1 Ma is a good age information for this event. For Portuguese granitoids, Pinto (1985) establishes a Westphalian age group (305 ± 5 Ma) that includes the age range of 300–311 Ma proposed in this study for late- and late- to post-D3 granitoid magmatism.

The post-D3 (syn-D4) granitoids dated in this study were three of the four granite units that constitute the Peneda–Gerês pluton. Zircon and monazite age data of the Gerês granite indicate a crystallization age of 297 ± 7 Ma and 296 ± 2 Ma, respec-

tively. Zircon data yielded a crystallization age of 290 ± 2.5 Ma for the Paufito granite and a minimum emplacement age of 280 ± 5 Ma for the Carris granite (Fig. 7). Field relations indicate that all four granites of the Peneda–Gerês massif are subcontemporaneous. The age difference between the Gerês and Paufito granites seems to indicate that the geochemically distinct Gerês granite represents a first magmatic pulse that was immediately followed by the intrusion of the magma that originated the other granites. The Stephanian age group (290 ± 5 Ma) defined by Pinto (1985) includes the 290–296 Ma range established for the studied post-D3 granitoids. For the Peneda–Gerês pluton other age interpretations are available from Rb–Sr whole-rock data. The ages obtained for the Gerês granite were 287 ± 4 Ma (MSWD = 0.3) (Priem et al., 1984), 293 ± 8 Ma (MSWD = 0.45) (Neiva, 1993a,b) and 296 ± 6 Ma (MSWD = 0.08) (Mendes et al., in preparation). These are similar to the zircon and monazite U–Pb ages, taking into account the ages and respective

errors. For the Carris granite the only Rb–Sr age available is of 302 ± 4 Ma (MSWD = 1.16) (Neiva, 1993b). For the Paufito and Illa granites a good quality isochron of 292 ± 6 Ma (MSWD = 0.26) (Mendes et al., in preparation) was obtained and tends to confirm the slightly younger crystallization age of the Paufito and Illa granites relatively to the surrounding Gerês granite.

The granitoids emplaced during the post-collisional stage of the Hercynian orogeny (syn- to post-D3, the last ductile deformation phase) are predominant in the CIZ. They show variable petrographic and compositional characteristics, the biotite-dominant granitoids being the most abundant. The following chronology is proposed for these syn- to post-tectonic granitoids, based on the U–Pb isotope data presented in this study (Fig. 7):

(1) Syn-D3 biotite granitoids, 313–319 Ma. Their chemical and Sr–Nd isotopic data reveal calc-alkaline and aluminopotassic affinities, with hybrid (interaction of mantle and crust magmas) and deep anatectic genesis (Simões et al., 1997b; study in progress).

(2) Late-D3 biotite-dominant granitoids, 306–311 Ma. On the basis of chemical and Sr–Nd isotopic studies, these granites are related to subalkaline (monzonitic) and aluminopotassic series, being originated by hybrid and anatectic processes, respectively (Dias et al., 1992; Dias and Leterrier, 1993, 1994; study in progress).

(3) Late- to post-D3 granitoids, around 300 Ma. They are aluminopotassic and strongly peraluminous granitoids of upper crust anatectic origin (Dias et al., 1992).

(4) Post-D3 granitoids, 290–296 Ma. They present a subalkaline ferro-potassic affinity and originate essentially by hybridization mechanisms involving alkaline and calc-alkaline magmas (Mendes et al., 1997; study in progress).

These chronological data indicate that the major post-collisional granitic intrusions of the CIZ in Northern Portugal were emplaced within a rather narrow time span (ca. 300–320 Ma) which corresponds to the time interval of the last regional ductile deformation phase (D3). For the two-mica S. Ovídio granite (Northern Portugal), emplaced after the D2 and before the D3 deformation phases, an emplacement age of 333 Ma was proposed (Dias and Boul-

lier, 1985; Dias, 1987). This is in agreement with the lower limit proposed here for the D3 deformation. The time interval of ca. 300–320 Ma for the D3 in the CIZ also agrees with the timing proposed by Ferreira et al. (1987a) (proposal modified by Noronha et al., 1979; Pinto et al., 1987). In continuity, less voluminous intrusions characterized by a subalkaline ferro-potassic affinity were emplaced. This granitic plutonism (ca. 290–296 Ma) is controlled by the fragile phase of deformation D4 in relation with the late-Hercynian crustal extension that began at ca. 300 Ma. Thus a rapid and drastic change in both the nature of magma protoliths and the tectonic regime of the crust occurred at this time.

Acknowledgements

References

Bard, J.P., Burg, J.P., Matte, P., Ribeiro, A., 1980. La chaîne hercynienne d'Europe occidentale en termes de tectonique des plaques. Mém. BRGM 108, 233–246.

Beetsma, J.J., 1995. The Late Proterozoic/Paleozoic and Hercynian crustal evolution of the Iberian Massif, N. Portugal. PhD Thesis, Vrije Universiteit Amsterdam, 223 pp.

Burg, J.P., Van den Driessche, J., Brun, J.P., 1994. Syn- to post-thickening extension: mode and consequences. C. R. Acad. Sci. Paris 319, 1019–1032, série II.

Debon, F., Le Fort, P., 1983. A chemical–mineralogical classification of common plutonic rocks and associations. Trans. R. Soc. Edinburgh, Earth Sciences 73, 135–149.

Dias, G., 1987. Mineralogia e petrologia de granitos Hercínicos associados a mineralizações filonianas de Sn–W, (Minho, Portugal). PhD Thesis, unpublished, Universidade do Minho, Portugal, 304 pp.

Dias, G., Boullier, A.M., 1985. Évolution tectonique, métamorphique et plutonique d'un secteur de la chaîne hercynienne ibérique (Ponte de Lima, Nord du Portugal). Bull. Soc. Géol. France 8, 423–434.

Dias, G., Leterrier, J., 1993. Cronologia e petrogénese de

granitóides biotíticos tardi-hercínicos (Minho, Portugal). Estudo isotópico Rb–Sr e Sm–Nd. Publ. Mus. Lab. Min. Geol. Univ. Porto 3, 369–373.

Dias, G., Leterrier, J., 1994. The genesis of felsic–mafic plutonic associations: a Sr and Nd isotopic study of the Hercynian Braga Granitoid Massif (Northern Portugal). Lithos 32, 207–223.

Dias, G., Leterrier, J., Ferreira, N., Lopes Nunes, J.E., 1992. Les granitoïdes biotitiques syn- à tardi-hercyniens de la région de Braga (Nord Portugal). Typologie chimico–minéralogique et implications pétrogénétiques. C. R. Acad. Sci. Paris 314, 675–681, série II.

Diez Balda, M.A., Vegas, R., Gonzalez Lodeiro, F., 1990. Structure of autochtonous sequences of Central Iberian Zone. In: Dallmeyer, R.D., Martínez, E. (Eds.), Pre-Mesozoic Geology of Iberia. Springer-Verlag, Berlin, Germany, pp. 172–188.

Evensen, N.M., Hamilton, P.J., O'Nions, R.K., 1978. Rare-earth abundances in chondritic meteorites. Geochim. Cosmochim. Acta 42, 1199–1212.

Ferreira, N., Iglesias, M., Noronha, F., Pereira, E., Ribeiro, A., Ribeiro, M.L., 1987a. Granitóides da Zona Centro Ibérica e seu enquadramento geodinâmico. In: Bea, F., Carnicero, A., Gonzalo, J.C., López Plaza, M., Rodriguez Alonso, M.D. (Eds.), Geologia de los Granitoides y Rocas Asociadas del Macizo Hespérico. Ed. Rueda, Madrid, pp. 37–51.

Ferreira, N., Macedo, C.A.R., Sousa, M.B., 1987b. Cronostratigrafia dos granitos da região de Moimenta da Beira–Tabuaço–Penedono. Publ. Mus. Lab. Min. Geol. Univ. Porto 1, 287–302.

Ferreira, N., Dias, G., Leterrier, J., Lopes Nunes, J.E., 1993. Rochas ígneas hercínicas da região de Braga–Vieira do Minho (NW de Portugal): cartografia geológica, tipologia granítica e petrogénese. Publ. Mus. Lab. Min. Geol. Univ. Porto 3, 45–49.

Govindaraju, K., Mevelle, G., 1987. Fully automated dissolution and separation methods for inductively coupled plasma atomic emission spectrometry rock analysis. Application to the determination of rare earth elements. J. Anal. Atom. Spectrom. 2, 615–621.

Iglesias, M., Ribeiro, A., 1981. Zones de cisaillement ductile dans l'arc ibéro-armoricain. Comun. Serv. Geol. de Portugal 67, 85–87.

Julivert, M., Fontboté, J., Ribeiro, A., Conde, L., 1974. Mapa tectónico de la Península Ibérica y Baleares, escala 1/1,000,000. Inst. Geol. Min. España, 113 pp.

Krogh, T.E., 1973. A low contamination method for the hydrothermal decomposition of zircon and extraction of U and Pb for isotopic age determinations. Geochim. Cosmochim. Acta 37, 485–494.

Krogh, T.E., 1982. Improved accuracy of U–Pb zircon ages by the creation of more concordant systems using an air abrasion technique. Geochim. Cosmochim. Acta 46, 637–649.

Lagarde, J.L., Capdevila, R., Fourcade, S., 1992. Granites et collision continentale: l'exemple des granitoïdes carbonifères dans la chaîne hercynienne ouest-européenne. Bull. Soc. Géol. France 163, 597–610.

La Roche, H., Stussi, J.M., Chauris, L., 1980. Les granites à deux micas hercyniens français. Essai de cartographie et de corrélations géochimiques appuyés sur une banque de données. Implications pétrologiques et métallogéniques. Sci. Terre, Nancy 24, 5–121.

Lotze, F., 1945. Zur Gliederung der Varisziden der Iberischen Meseta. Geotekt. Forsch. 6, 78–82.

Ludwig, K.R., 1987. Isoplot 200, a plotting and regression program for isotope geochemists, for use with HP series 200 computers. US Geol. Surv. Open File Rep., 45 pp.

Martins, M.E.R., 1997. Geologia, petrologia e geoquímica dos granitóides hercínicos da região de Lamego (Norte de Portugal). PhD Thesis, unpublished, Universidade de Aveiro, Portugal, 287 pp.

Matte, Ph., 1986. La chaîne varisque parmi les chaînes plaéozoïques péri atlantiques, modèle d'évolution et position des grands blocs continentaux au Permo–Carbonifère. Bull. Soc. Géol. France 2, 9–24.

Mendes, A.C., 1994. O maciço granítico de Peneda–Gerês: petrologia, mineralogia e geoquímica. Provas de APCC, unpublished, Universidade do Minho, Portugal, 157 pp.

Mendes, A.C., Dias, G., 1996. Petrology and geochemistry of late-Hercynian subalkaline plutonism in the Central Iberian Zone: the Peneda–Gerês granitic massif. C. R. Acad. Sci. Paris 323, 665–672, série IIa.

Mendes, A.C., Pupin, J.P., Dias, G., 1997. Petrogénese do maciço subalcalino de Peneda–Gerês (NW Península Ibérica): evidências a partir da estrutura interna e geoquímica de elementos traço de zircões. X Semana de Geoquímica e IV Congresso de Geoquímica dos Países de Língua Portuguesa. Braga, Portugal, pp. 99–102.

Montenegro de Andrade, M., Noronha, F., Rocha, A., 1986. Carta geológica de Guimarães (folha 9-B), escala 1/50,000. Serv. Geol. de Portugal, Lisboa.

Nachit, H., Razafimahefa, N., Stussi, J.M., Carron, J.P., 1985. Composition chimique des biotites et typologie magmatique des granitoïdes. C. R. Acad. Sci. Paris 301, 813–818.

Neiva, A.M.R., 1993a. Geoquímica de granitos e seus minerais da Serra do Gerês, Norte de Portugal. Publ. Mus. Lab. Min. Geol. Univ. Porto 3, 137–139.

Neiva, A.M.R., 1993b. Geochemistry of granites and their minerals from Gerez mountain, Northern Portugal. Chem. Erde. 53, 227–258.

Nemchin, A.A., Pidgeon, R.T., Wilde, S.A., 1994. Timing of late Archean granulite facies metamorphism in the southwestern Yilgarn Craton of Western Australia: evidence from U–Pb ages of zircons in mafic granulites. Precambr. Res. 68, 307–321.

Noronha, F., Ramos, J.M.F., Rebelo, J.A., Ribeiro, A., Ribeiro, M.L., 1979. Essai de corrélation des phases de déformation hercynienne dans le Nord–Ouest Péninsulaire. Bol. Soc. Geol. Portugal 21, 227–237.

Parrish, R.R., Roddick, J.C., Loveridge, W.D., Sullivan, R.W., 1987. Uranium–lead analytical techniques at the Geochronology Laboratory, Geological Survey of Canada. Radiogenic Age and Isotopic Studies: Report 1. Geol. Surv. Canada, Paper 87-2, 3–7.

Pereira, E. (coord.), 1992. Carta geológica de Portugal. Escala

1/200,000. Notícia Explicativa da Folha 1. Serv. Geol. de Portugal, Lisboa, 83 pp.

Pereira, E., Ribeiro, A., Meireles, C., 1993. Cisalhamentos hercínicos e controlo das mineralizações de Sn–W, Au e U na Zona Centro-Ibérica, em Portugal. Cuad. Lab. Xeol. Laxe 18, 89–119.

Pinto, M.S., 1985. Escala geocronológica de granitóides portugueses ante-mesozóicos: uma proposta. Mems. Nots. Publ. Mus. Lab. Min. Geol. Univ. Coimbra 99, 157–166.

Pinto, M.S., Casquet, C., Ibarrola, E., Corretgé, L.G., Portugal Ferreira, M., 1987. Síntese geocronológica dos granitóides do maciço hespérico. In: Bea, F., Carnicero, A., Gonzalo, J.C., López Plaza, M., Rodriguez Alonso, M.D. (Eds.), Geologia de los granitoides y rocas asociadas del Macizo Hespérico. Ed. Rueda, Madrid, pp. 69–86.

Priem, H.N.A., Schermerhorn, L.J.G., Boelrijk, N.A.I.M., Hebeda, E.H., 1984. Rb–Sr geochronology of Variscan granitoids in the tin–tungsten province of northern Portugal: a progress report. Terra Cognita 4, 212–213.

Pupin, J.P., 1980. Zircon and granite petrology. Contrib. Mineral. Petrol. 73, 207–220.

Pupin, J.P., 1981. A propos des granites potassiques. C. R. Acad. Sci. Paris 292, 405–408.

Pupin, J.P., 1988. Granites as indicators in paleogeodynamics. Rend. Soc. Ital. Mineral. Petrol. 43 (2), 237–262.

Rey, P., Burg, J.P., Casey, M., 1997. The Scandinavian Caledonides and their relationship to the Variscan belt. In: Burg, J.P., Ford, M. (Eds.), Orogeny Through Time. Geological Society Special Publication, 121, pp. 179–200.

Ribeiro, A., 1974. Contribution à l'étude tectonique de Trás-os-Montes oriental. Mem. Serv. Geol. Portugal 24, 168.

Ribeiro, A., Iglesias, M., Ribeiro, M.L., Pereira, E., 1983. Modèle géodynamique des Hercynides Ibériques. Comun. Serv. Geol. Portugal 69, 291–293.

Ribeiro, A., Pereira, E., Dias, R., 1990a. Structure in the NW of the Iberian Peninsula. In: Dallmeyer, R.D., Martínez, E. (Eds.), Pre-Mesozoic Geology of Iberia. Springer-Verlag, Berlin, pp. 220–236.

Ribeiro, A., Quesada, C., Dallmeyer, R.D., 1990b. Geodynamic evolution of the Iberian Massif. In: Dallmeyer, R.D., Martínez, E. (Eds.), Pre-Mesozoic Geology of Iberia. Springer-Verlag, Berlin, pp. 399–409.

Rossi, P., Chevremont, P., 1987. Classification des associations magmatiques granitoïdes. Géochronique 21, 14–18.

Simões, P.P., Dias, G., Leterrier, J., 1997a. Petrogénese de granitóides hercínicos biotíticos associados ao cisalhamento Vigo-Régua (Norte de Portugal). I Congresso Ibérico de Geoquímica e VII Congresso de Geoquímica de Espanha, Soria, Spain, pp. 528–534.

Simões, P.P., Pupin, J.P., Dias, G., 1997b. Utilização do zircão como indicador genético e evolutivo em granitóides hercínicos biotíticos associados ao cisalhamento Vigo-Régua (Norte de Portugal). X Semana de Geoquímica e IV Congresso de Geoquímica dos Países de Língua Portuguesa. Braga, Portugal, pp. 147–150.

Stacey, J.S., Kramers, J.D., 1975. Approximation of terrestrial lead isotope evolution by a two-stage model. Earth Planet. Sci. Lett. 26, 207–221.

Steiger, R.H., Jäger, E., 1977. Convention of the use of decay constants in geo- and cosmochronology. Earth Planet. Sci. Lett. 36, 359–362.